

Floquet-Bloch Oscillations and Intraband Zener Tunneling in an Oblique Spacetime Crystal

Qiang Gao and Qian Niu

Department of Physics, University of Texas at Austin, Texas, USA

(Dated: June 15, 2022)

We study an oblique spacetime crystal realized by a monoatomic crystal in which a sound wave propagates, and analyze its quasienergy band structure originating from a tight-binding Bloch band for the static crystal. We investigate Floquet-Bloch oscillations under an external field, and discover intraband Zener tunneling which otherwise cannot occur for a rectangular spacetime crystal with separate space and time periodicities. The intraband tunneling changes the band topology of the oblique spacetime crystal, resulting in the possibility of a quantum acoustoelectric generator that converts energy between the sound wave and a DC electric field in quantized units.

Introduction.— Periodically driven quantum systems have a long history of study in physics, and have emerged in recent years as a new play ground for novel topological properties [1–3] and quantum materials engineering [4]. There are also discussions on the tantalizing possibility of spontaneous formation of time crystals [5–8] and spacetime crystals [9], adding new excitements to this field. However, there are still much to be explored, and there are challenges in understanding the electronic dynamics in such systems [10, 11].

According to a recently reported symmetry classification [12], Spacetime crystals fall into rectangular and oblique categories, depending on whether the system has separate translational symmetries in space and time. Here we present an example for the latter, a monoatomic crystal in which a single mode of sound wave propagates. One can still make a Floquet-Bloch analysis, but quasienergies and momenta are now defined modulo an oblique Brillouin zone, and the usual concepts of Bloch oscillations and Zener tunneling for Bloch bands can be essentially modified. We show intraband Zener tunneling can occur under an external field, which effectively changes the topology of a band, leading to a novel mechanism for a quantum acousto-electric generator that converts energy between the sound mode and a dc electric field.

Floquet-Bloch analysis for an oblique spacetime crystal.— The band theory goes quite parallel to that for a rectangular spacetime crystal [13]. The oblique spacetime crystal considered here is a mono-atomic crystal with sound waves propagating though it:

$$H(\mathbf{x}, t) = \frac{-\hbar^2}{2M} \nabla_{\mathbf{x}}^2 + \sum_{\mathbf{R}} V(\mathbf{x} - \tilde{\mathbf{R}}) \quad (1)$$

with the atomic position being time-dependent $\tilde{\mathbf{R}} = \mathbf{R} - \mathbf{A} \cos(\boldsymbol{\kappa} \cdot \mathbf{R} - \Omega t)$. Here the $(\boldsymbol{\kappa}, \Omega)$ is the momentum and frequency of that sound wave, $|\mathbf{A}|$ is the oscillation amplitude and $\mathbf{R} = n_1 \mathbf{a}_1 + n_2 \mathbf{a}_2 + n_3 \mathbf{a}_3$ labels the lattice sites. This Hamiltonian has the following translational symmetries: $H(\mathbf{x}, t + 2\pi/\Omega) = H(\mathbf{x}, t) = H(\mathbf{x} + \mathbf{R}, t + \boldsymbol{\kappa} \cdot \mathbf{R}/\Omega)$, which defines an oblique Spacetime lattice with non-

orthogonal lattice vectors being $(\mathbf{0}, \frac{2\pi}{\Omega})$ and $(\mathbf{R}, \frac{\boldsymbol{\kappa} \cdot \mathbf{R}}{\Omega})$. This then determines the reciprocal (energy-momentum) lattice structure to be also oblique which is characterized by vectors: $(\boldsymbol{\kappa}, \Omega)$ and $(\mathbf{G}, 0)$, with \mathbf{G} being the reciprocal lattice vector of the corresponding static crystal [14].

The Floquet-Bloch eigenstates are solutions of the time-dependent Schrodinger equation:

$$H(\mathbf{x}, t) |\Psi(\mathbf{x}, t)\rangle = i\hbar \partial_t |\Psi(\mathbf{x}, t)\rangle, \quad (2)$$

and satisfy the conditions: . We will assume that $(|\mathbf{A}| \ll \text{lattice constants})$, and consider the effect of lattice vibration to leading orders in the amplitude \mathbf{A} : $H(\mathbf{x}, t) = H_0(\mathbf{x}) + \mathbf{A} \cdot \mathbf{H}_1(\mathbf{x}, t) + \dots$, where H_0 is the Hamiltonian of the corresponding static lattice. To simplify matters, we assume that the electrons are all in the lowest Bloch band of the static lattice, which is well-separated from other bands energetically so that mixing with them can still be ignored when the lattice vibration is turned on.

Under these conditions, lattice vibrations can still mix a Bloch state $\{|\psi_{\mathbf{k}}(\mathbf{x})\rangle\}$ of energy $\omega_g(\mathbf{k})$ in the lowest band with others of the same band which differ by integer multiple of the phonon energy and momentum $(\Omega, \boldsymbol{\kappa})$. In other words, we can choose the basis states to be the phonon replica of a Bloch state:

$$\{|\Phi_{n,\mathbf{k}}(\mathbf{x}, t)\rangle\} \equiv e^{-in\Omega t} |\psi_{\mathbf{k}+n\boldsymbol{\kappa}}(\mathbf{x})\rangle, \quad (3)$$

where n is the replica index. This basis can be made orthonormal under a new inner product defined as

$$\langle\langle \phi(\mathbf{x}, t) | \psi(\mathbf{x}, t) \rangle\rangle \equiv \frac{1}{T} \int_0^T dt \int d\mathbf{x} \phi^*(\mathbf{x}, t) \psi(\mathbf{x}, t) \quad (4)$$

where $T = 2\pi/\Omega$ is the time period.

Having the phonon replica basis, we can then expand the real solution of Eq.(2) as: $|\Phi_{\omega}(\mathbf{x}, t)\rangle = \sum_{n,\mathbf{k}} e^{-i\omega t} f_{\mathbf{k}}^n |\Phi_{n,\mathbf{k}}(\mathbf{x}, t)\rangle$ where ω is the so-called quasi-energy and the summation is over both momentum \mathbf{k} and index n , which indicates that the conservation of lattice momentum and energy is broken. Instead, we have a weaker conservation law: the conservation of quasi-momentum, that the initial and final momentum can be

differed by an integer multiple of κ [15]. By utilizing this property, we can drop the summation over \mathbf{k} in $\Phi_\omega(\mathbf{x}, t)$ and use both quasi-energy and quasi-momentum as characterizations for the state:

$$|\Phi_{\omega(\mathbf{k})}(\mathbf{x}, t)\rangle = \sum_n e^{-i\omega(\mathbf{k})t} f_{\mathbf{k}}^n |\Phi_{n, \mathbf{k}}(\mathbf{x}, t)\rangle. \quad (5)$$

Then plugging this expansion into the time-dependent Schrodinger Equation Eq.(2), we can obtain a matrix equation about the $f_{\mathbf{k}}^n$: $\sum_n \mathcal{H}_{m, n}(\mathbf{k}) f_{\mathbf{k}}^n = \hbar\omega(\mathbf{k}) f_{\mathbf{k}}^m$ where matrix $\mathcal{H}(\mathbf{k})$ is the kernel of original Hamiltonian in the Floquet-Bloch basis with element defined as

$$\mathcal{H}_{m, n} \equiv \langle\langle \Phi_{m, \mathbf{k}}(\mathbf{x}, t) | H(\mathbf{x}, t) | \Phi_{n, \mathbf{k}}(\mathbf{x}, t) \rangle\rangle - \hbar n \Omega \delta_{mn}. \quad (6)$$

A simple observation is when $\mathbf{A} = \mathbf{0}$, the matrix \mathcal{H} is simply a diagonal matrix: $\mathcal{H}_{m, n} = \hbar(\omega_g(\mathbf{k} + n\kappa) - n\Omega) \delta_{mn}$ which leads to the Floquet band dispersion for the empty lattice: $\omega_n(\mathbf{k}) = \omega_g(\mathbf{k} + n\kappa) - n\Omega$ (see for example the dashed curves in Fig.1). Then as turning on the perturbation, we will have nonzero off-diagonal elements in the matrix \mathcal{H} , which introduces interactions between unperturbed replicas and opens the gap. A detailed evaluation for matrix elements of \mathcal{H} for a perturbed case is presented in [15]. In the rest of this letter, we will only focus on the (1+1)D system.

Fig.1 shows a typical Floquet-Bloch band dispersion in (1+1)D using a simple set-up [16]. The dashed curves are the unperturbed bands with no oscillation, and we can see they are nothing but replicas of the original ‘cos’-shape Bloch band. The solid curves are the band dispersion under time-dependent perturbation. The red shadowed area stands for the Brillouin Zone of the Oblique Spacetime Crystal characterized by two reciprocal lattice vector: $(G = 2\pi/a, 0)$ and (κ, Ω) . Without loss of physics, we take the $(n = 0)$ band $\omega_0(k)$ as our first Brillouin Zone and all others are replicas.

Floquet-Bloch Oscillations and Corresponding Band Topology.— Based on the Floquet-Bloch band theory, we can study the dynamics of electrons under external forces. If we apply an electric field E to the spacetime crystal, the quasi-momentum of the electron will evolve as $k \rightarrow k' = k + e\mathbb{A}/\hbar$ where $\mathbb{A} = -Et$ is the vector potential. The changing momentum over time also affects the position of the electron which can be determined using perturbation method. The motion of the electron then obeys the following equations [15]

$$\dot{k} = -\frac{eE}{\hbar}, \quad \dot{x} = \frac{\partial \omega_n(k)}{\partial k}, \quad (7)$$

which is similar to the case in Bloch crystals[17]. In periodic system, the motion of electrons should also manifest its periodicity. Given the band structure in Fig.1, there is an apparent periodicity in the quasi-energy $\omega(k)$ over k : $\omega_n(k + 2\pi/a) = \omega_n(k)$, which implies, according to the equations of motion, that the velocity of electrons is also

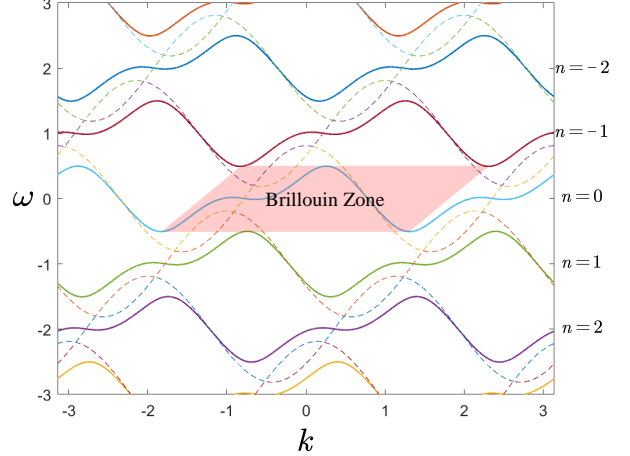


FIG. 1: Floquet-Bloch band structure for the (1+1)D oblique Spacetime crystal modeled by Eq.(6), originating from the lowest Bloch band (dashed curves repeated over the Brillouin zone) of the unperturbed system. The quasienergy dispersion (solid curves) is calculated when a single mode of sound wave is turned on to a finite amplitude [16]. The labels on the right vertical axis are the indices of replica of the same single band as defined within the Brillouin zone.

periodic in k with oscillating period $\frac{\hbar}{eE}G$. That is the so-called Bloch oscillation originated from the periodic structure in space [18].

Similar to the Bloch oscillation, the periodic structure in time will also impose periodicity to the motion of electrons. The periodicity in time is again reflected in the quasi-energy: $\omega_n(k + \kappa) = \omega_n(k) + \Omega$ [19] and $\omega_n(k + 2\pi/a \pm \kappa) = \omega_n(k) \pm \Omega$, which will, in principle, lead to new types of oscillation in electron’s velocity with periods being $\frac{\hbar}{eE}\kappa$ and $\frac{\hbar}{eE}(G \pm \kappa)$, respectively. These two possible oscillations together with the Bloch oscillation are the Floquet-Bloch oscillations.

Back to band picture, there are different band topologies associated to those oscillations. In order to see that, we need to project the Brillouin zone onto a spacetime torus (see Ref. [15] for more details).

As shown in Fig.2 (a,b,c), there are generically three types of band topology characterized by the winding numbers N_ω and N_k along the directions of two reciprocal lattice vectors: Fig.2 (a) shows the most trivial band structure with winding number $N_\omega = 0, N_k = 1$ and it implicates the Bloch oscillation with period $\propto G$; Fig.2 (b) gives the first non-trivial topology where $N_\omega = 1, N_k = 0$ and it represents the Floquet-Bloch oscillation with period $\propto \kappa$; Fig.2 (c) is the combination of the previous two cases which has winding number $N_\omega = -1, N_k = 1$ (case with $N_\omega = N_k = 1$ is similar) and stands for the Floquet-Bloch Oscillation with period $\propto G - \kappa$ (or $G + \kappa$ in the case where $N_\omega = N_k = 1$). In other words, the Floquet-Bloch oscillation period is proportional to $N_\omega \kappa + N_k G$. It is noteworthy that the

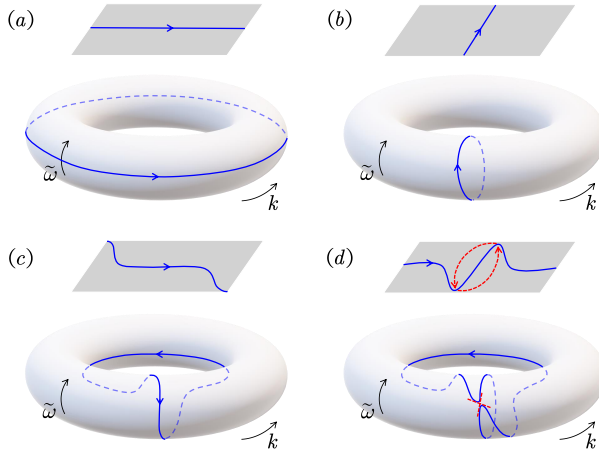


FIG. 2: Topology of band dispersions (blue curves) as seen on the torus of the Brillouin zone, which wraps around in the directions of the two reciprocal lattice vectors: $\tilde{\omega} = (\kappa, \Omega)$ and $\mathbf{k} = (G, 0)$. Panel (a) corresponds to the class shown in Fig.(1), Panel (b) is a class that has not been seen yet. Panel (c) corresponds to typical edge states of topological Floquet insulator in higher dimension [3]. Panel (d) has the same topology as in (a), but with a near self-crossing on the torus. When intraband Zener tunneling occurs under an external force, this band effectively breaks up into two corresponding to those of Panel (b,c).

periodicity in Fig.2 (a) and (b) correspond to two physical processes: Bragg Scattering and Brillouin Scattering, respectively, and that the one in Fig.2 (c) is a combination of both two scatterings.

However, band structures in Fig.2 (b,c) are highly non-trivial. For the band structure in Fig.2 (b), it is impossible to exist in a system with $\kappa = 0$ (rectangular spacetime crystal) since it will inevitably lead to an infinitely large group velocity of electrons ($\dot{x} \rightarrow \infty$) as $\kappa \rightarrow 0$. So, topology with winding number $N_\omega = \pm 1, N_k = 0$ is mechanically forbidden in rectangular spacetime crystals and is therefore only possible in an oblique spacetime crystal where the group velocity is of the order of the sound velocity Ω/κ . Then for the band structure in Fig.2 (c), it commonly exists as the edge state of a higher dimensional system like the edge of (2+1)D spacetime crystal [3]. Those non-trivialities always suggest difficulties of experimental realizations.

Despite the potential difficulties, we can still achieve those two non-trivial topologies through a very special shortcut. As shown in Fig.2 (d), the band structure is topologically the same as the one in Fig.2 (a) which is trivial, but it has a unique feature where two well-separated points in one band are instead very close to each other when they are projected onto the surface of the spacetime torus. Now if the electron can hop from one point to another point, then the original band structure will be tailored into two separate parts, which reproduce the same topology as in Fig.2 (b) and (c). Fortunately,

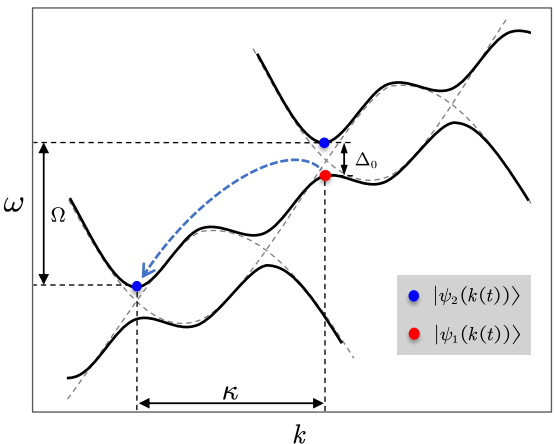


FIG. 3: Zener tunneling across a small gap Δ_0 occurs when the momentum k changes with time under an external field just like for Bloch states. However, since the different bands are really replicas of the same Floquet-Bloch band, shifted by the phonon energy and momentum (Ω, κ) , Zener tunneling in the present context is actually an intraband process indicated by the dashed arrow.

the unique band structure can be realized through a relatively simple set-up and the intraband hopping can also be achieved through intraband Zener tunneling which will be discussed below.

Intraband Zener Tunneling.— The intraband Zener tunneling is an analog of Zener tunneling process happened in Floquet system. Previous works on Zener tunneling in Floquet system were mainly focusing on the atomic states and also did not look up on the effects in the context of the oblique spacetime lattice [20–22]. In this Section, we will propose an intraband Zener tunneling happened in oblique spacetime crystals. The key idea is that given two eigen-states $|\psi_1(k(t))\rangle$ and $|\psi_2(k(t))\rangle$:

$$|\psi_1(k(t))\rangle = e^{-i\epsilon_1 t} \sum_n f_{k(t)}^n |\Phi_{n,k(t)}(x, t)\rangle \quad (8)$$

$$|\psi_2(k(t))\rangle = e^{-i\epsilon_2 t} \sum_n f_{k(t)-\kappa}^n |\Phi_{n-1,k(t)}(x, t)\rangle,$$

sitting on two bands (replicas) labeled by 1 and 2, they have quasi-energies $\epsilon_1 = \omega(k(t))$ and $\epsilon_2 = \omega(k(t) - \kappa) + \Omega$, respectively. One can check that $|\psi_1(k(t))\rangle$ and $|\psi_2(k(t))\rangle$ are orthonormal to each other ($\langle\langle\langle\psi_i(k(t))|\psi_j(k(t))\rangle\rangle\rangle = \delta_{ij}$). In Fig.3, we depict these two states using different colors. At some k point, they are close to each other (in the sense of repeated zone picture), where a tunneling process may happen if a sufficiently large driven force is applied.

To find out the possibility of tunnelling electrons between $|\psi_1(k(t))\rangle$ and $|\psi_2(k(t))\rangle$, we can calculate the tunneling rate through this channel. By applying an electric field E , as described by Eq.(7), those two states will move along k axis. In this case, the real wavefunction

is a linear combination of two eigen-states: $|\Phi(t)\rangle = C_1(t)|\psi_1(k(t))\rangle + C_2(t)|\psi_2(k(t))\rangle$, where we assume that $C_{1,2}(t)$ are slow varying in time compared to the Floquet period, $2\pi/\Omega$. Now, plugging the wavefunction into the time-dependent Schrodinger Equation, we obtain the following differential equation related to $C_{1,2}$ [15]:

$$i\hbar \frac{\partial}{\partial t} \begin{bmatrix} C_1 \\ C_2 \end{bmatrix} - eE \begin{bmatrix} \mathcal{A}_{11} & \mathcal{A}_{12} \\ \mathcal{A}_{21} & \mathcal{A}_{22} \end{bmatrix} \begin{bmatrix} C_1 \\ C_2 \end{bmatrix} = \begin{bmatrix} \epsilon_1 & 0 \\ 0 & \epsilon_2 \end{bmatrix} \begin{bmatrix} C_1 \\ C_2 \end{bmatrix} \quad (9)$$

where $\mathcal{A}_{ij} \equiv \langle\langle \psi_i(k(t)) | (i\partial_k + x) | \psi_j(k(t)) \rangle\rangle$ is the multi-band Floquet-type Berry connection. This result has the same form as in Bloch crystals but with modified Berry connections. In our concern, the set-up is that initially, the state is on band 1, which means $C_1(0) = 1$ and $C_2(0) = 0$ and then let the system evolves. For Spacetime crystal, \mathcal{A}_{ij} generically has two contributions:

$$\mathcal{A}_{ij} = i \sum_n (f_j)^* \partial_k f_i + \sum_n (f_j)^* f_i \mathcal{A}_{k+n\kappa} \quad (10)$$

where $f_1 \rightarrow f_k^n$ and $f_2 \rightarrow f_{k-\kappa}^{n+1}$. The first term is the Floquet contribution while the second term is the modified Bloch contribution with $\mathcal{A}_{k+n\kappa}$ being the usual Berry connection. For the Floquet-Bloch system generated by a single Bloch band well-separated from all other bands, this Bloch contribution is numerically small and neglectable. Then $\mathcal{A}_{ij}(k)$ has only the Floquet contribution that comes solely from the time variations, which allows us to consider only the kernel $\mathcal{H}(k)$ in Eq.(6).

Since our main concern is the adjacent two replicas labeled by 1 and 2, we can approximate the infinitely large kernel matrix by the following 2 by 2 matrix:

$$h(k) = \begin{bmatrix} \mathcal{E}_2(k) & \Delta(k)/2 \\ \Delta^*(k)/2 & \mathcal{E}_1(k) \end{bmatrix} \quad (11)$$

where $\mathcal{E}_{i,j}(k)$ are the diagonal elements that have crossing point at $k = k_0$, and $\Delta(k)$ is the generically k -dependent gap function. Now if we look close to the band crossing point and expand the $h(k)$ around that point then keep only the leading order in $(k - k_0)$, we end up with Zener's original two-level model with transition rate [23]:

$$\Gamma = |C_2(t \rightarrow \infty)|^2 = \exp \left(-\frac{\pi \Delta_0^2}{2eE\mu} \right), \quad (12)$$

where $\Delta_0 \equiv |\Delta(k_0)|$ (see also Fig.3) and $\mu \equiv \mathcal{E}'_1(k_0) - \mathcal{E}'_2(k_0)$. This result shows clearly that the intraband tunneling is possible under certain conditions.

Compared to the Bloch crystal, one of essential differences is that the tunneling happened in spacetime crystal only requires a quasi-momentum conservation, namely $k_i = k_f + \kappa$, instead of an exact conservation of lattice momentum. In other words, the intraband Zener tunneling happens along with the momentum shift, which can be interpreted as a normal Zener tunneling process

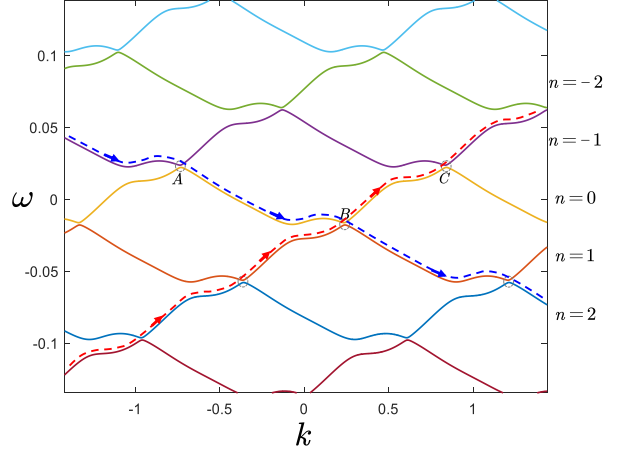


FIG. 4: Floquet-Bloch band structure with a very small gap of avoided crossing, calculated for the example of an oscillating Dirac Comb with oscillation amplitude $A = 0.16$ [15], can be used for the actions of a Quantum Acousto-Electric Generator. An electron in a state between A and B will be driven downward, continue the dashed-blue path by crossing the gap at B and so on, with a dc current against the external field. On the other hand, an electron in a state between B and C will be driven upward and continue the red-dashed path by Zener tunneling across the gaps along the way, with a dc current along the external field. A quantum of phonon energy is absorbed from or delivered to the sound wave at each period of these processes.

associated with emission or absorption of a quantum of sound mode, (Ω, κ) .

Quantum Acousto-Electric Generator.— As the last part of achieving the system in Fig.2(d), we need to carefully engineer the spacetime crystal to have only one primary bandgap. The primary band gap is defined as the direct gap at which the tunneling process is most likely to happen. Here we propose a promising system called Oscillating Dirac Comb [15] whose band structure is shown in Fig.4, and as we can see, has only one tiny primary band gap within the Brillouin Zone. This particular band structure can also be used to construct a quantum acousto-electric generator which continuously converts energy between the sound wave and a DC electric field in quantized units.

The basic set-up is that given the band structure depicted in Fig.4, we apply an electric field to drive electrons. For the intraband Zener tunneling process, we can use the sudden limit that when $|eE| \gg \Delta_0^2/\mu$, the tunneling rate is unity ($\Gamma = 1$), while when $|eE| \ll \Delta_0^2/\mu$, the tunneling rate is zero ($\Gamma = 0$). Here the electric field acts like a switch turning on or off the tunneling. Then for the system to be an Acousto-Electric Generator, we need to track the electron displacement over time:

$$\Delta x = \int \dot{x} dt = \int \frac{\partial \omega(k)}{\partial k} \frac{dk}{i} = -\frac{\hbar}{eE} \Delta \omega \quad (13)$$

TABLE I: Quantum Acousto-Electric Generator: the properties of three different processes.

Electric Field Strength	$ eE \ll \frac{\Delta_0^2}{\mu}$	$ eE \gg \Delta_0^2/\mu$
Electric Energy Gain/ \hbar	0	$\omega_A - \omega_B$
Oscillation Period in k	G	$G - \kappa$
Band Topology (N_k, N_ω)	(1,0)	(1,-1)
		(0,1)

where the equations of motion Eq.(7) are applied, and therefore the electric energy gain of an electron during this movement is $\Delta\mathcal{E} = -(-e)E\Delta x = -\hbar\Delta\omega$.

In Fig.4, points A , B , and C divide the ($n = 0$) band into two different segments: at segment AB , the quasi-energy is generically decreasing as k grows, while at segment BC , the quasi-energy is generically increasing. A tiny primary bandgap is associated with those three points where allows the tunneling process to happen. We then can tune the Electric Field Strength E to switch on or off the tunneling so that electrons can go specific paths. If $|eE| \ll \Delta_0^2/\mu$, the electron will adiabatically move from A to B and to C (equivalent to A), which corresponds to the process depicted in Fig.2(a). The electric energy gain associated with this process is $\hbar(\omega_A - \omega_C) = 0$. If $|eE| \gg \Delta_0^2/\mu$, a process described by Fig.2(d) is possible where the electron will move along the blue and red dashed lines shown in Fig.4 depending on electron's initial locations on the band. We summarize the characteristics of those three processes in Table I. The latter two cases have nonzero electric energy gains, capable of realizing the quantum acousto-electric generator.

The oscillation periods of three different processes can also be used as experimental signatures to determine whether one of those is happening and their dependence on the external electric field. Similarly, due to the relation between electronic current and electron velocity: $j = e\rho\dot{x}$ (ρ being the electron density), the three different periods also correspond to different frequencies in the AC part of the current j .

Acknowledgment.— The work is supported by NSF (EFMA-1641101) and Welch Foundation (F-1255).

Physics **10**, 387–408 (2019).

- [5] Wilczek, Frank. Quantum time crystals. *Phys. Rev. Lett.* **109**, 160401 (2012).
- [6] Else, Dominic V and Bauer, Bela and Nayak, Chetan. Floquet time crystals. *Phys. Rev. Lett.* **117**, 090402 (2016).
- [7] Zhang, Jiehang, et al. Observation of a discrete time crystal. *Nature* **543**, 217–220 (2017).
- [8] Autti, S and Eltsov, VB and Volovik, GE. Observation of a time quasicrystal and its transition to a superfluid time crystal. *Phys. Rev. Lett.* **120**, 215301 (2018).
- [9] Li, Tongcang, et al. Spacetime crystals of trapped ions. *Phys. Rev. Lett.* **109**, 163001 (2012).
- [10] Genske, Maximilian and Rosch, Achim. Floquet-Boltzmann equation for periodically driven Fermi systems. *Phys. Rev. A* **92**, 062108 (2015).
- [11] Messer, Michael, et al. Floquet dynamics in driven Fermi-Hubbard systems. *Phys. Rev. Lett.* **121**, 233603 (2018).
- [12] Xu, Shenglong and Wu, Congjun. Spacetime Crystal and Spacetime Group. *Phys. Rev. Lett.* **120**, 096401 (2018).
- [13] Gómez-León, Alvaro and Platero, Gloria. Floquet-Bloch theory and topology in periodically driven lattices. *Phys. Rev. Lett.* **110**, 200403 (2013).
- [14] Due to the convention of quantum mechanics that we always write the propagating phase factor as $e^{i\mathbf{k}\cdot\mathbf{x}-i\omega t}$, the space and time have naturally different signatures encoded. In this paper, the signature is set to be $(+, +, +; -)$ where the last entry stands for time. Then we can check that the reciprocal lattice vectors indeed fulfill: $-(\mathbf{0}, \frac{2\pi}{\Omega}) \cdot (\boldsymbol{\kappa}, \Omega) = (\mathbf{R}, \frac{\boldsymbol{\kappa} \cdot \mathbf{R}}{\Omega}) \cdot (\mathbf{G}, 0) = 2\pi$ and $(\mathbf{0}, \frac{2\pi}{\Omega}) \cdot (\mathbf{G}, 0) = (\mathbf{R}, \frac{\boldsymbol{\kappa} \cdot \mathbf{R}}{\Omega}) \cdot (\boldsymbol{\kappa}, \Omega) = 0$
- [15] See Supplementary Material
- [16] The set-up for obtaining the typical Floquet-Bloch band structure in Fig.1 is quite simple. We let the diagonal element of the kernel Matrix in Eq.(6) to be a ‘cos’-shape band dispersion: $\mathcal{H}_{n,n} = 2\beta \cos[(k+n\kappa)a] - n\Omega$, and then only consider constant off-diagonal terms: $\mathcal{H}_{n,n\pm 1} = \delta$. The parameters used are $\kappa = \Omega = 1$, $\beta = 0.8$, and $\delta = 0.3$
- [17] Marder, Michael P. Condensed matter physics. *John Wiley & Sons*.
- [18] Dahan, Maxime Ben, et al. Bloch oscillations of atoms in an optical potential. *Phys. Rev. Lett.* **76**, 4508 (1996).
- [19] This is equivalent to say that $\omega_n(k) = \omega_n(k + \kappa) - \Omega = \omega_{n+1}(k)$ which means that $\omega_n(k) \equiv \omega_0(k)$ for all n . Later, we will discuss that it requires a very unique band topology depicted in Fig.2(b).
- [20] Breuer, Heinz Peter and Holthaus, Martin. Quantum phases and Landau-Zener transitions in oscillating fields. *Physics Letters A* **140**, 507–512 (1989).
- [21] Hijii, Keigo and Miyashita, Seiji. Symmetry for the non-adiabatic transition in Floquet states. *Phys. Rev. A* **81**, 013403 (2010).
- [22] Rodriguez-Vega, M and Lentz, Meghan and Seradjeh, Babak. Floquet perturbation theory: formalism and application to low-frequency limit. *New Journal of Physics* **20**, 093022 (2018).
- [23] Zener, Clarence Non-adiabatic crossing of energy levels. *Proc. R. Soc. Lond. A* **137**, 696–702 (1932).

- [1] Rechtsman, Mikael C., et al. Photonic Floquet topological insulators. *Nature* **496**, 196–200 (2013).
- [2] Lindner, Netanel H and Refael, Gil and Galitski, Victor. Floquet topological insulator in semiconductor quantum wells. *Nat. Phys.* **7**, 490–495 (2011).
- [3] Yao, Shunyu and Yan, Zhongbo and Wang, Zhong. Topological invariants of Floquet systems: General formulation, special properties, and Floquet topological defects. *Phys. Rev. B* **96**, 195303 (2017).
- [4] Oka, Takashi and Kitamura, Sota. Floquet engineering of quantum materials. *Annual Review of Condensed Matter*